ORIGINAL ARTICLE

A C G publications

Rec. Nat. Prod. 17:1 (2023) 125-144

records of natural products

In Silico Study of Natural Xanthones as Potential Inhibitors of Alpha-Glucosidase and Alpha-Amylase

Michaella Yosephine [1], Isa Anshori [1], Muhammad Miftah Jauhar [2*], Putri Hawa Syaifie [2], Adzani Gaisani Arda [2], Azza Hanif Harisna [2], Dwi Wahyu Nugroho [2] and Etik Mardliyati [3]

[1]*Biomedical Engineering Department, School of Electrical Engineering and Informatics, Bandung Institute of Technology, Bandung, Indonesia*

[2] *Nano Center Indonesia, Jl. PUSPIPTEK, South Tangerang, Banten, 15314, Indonesia*

[3] *Research Center for Vaccine and Drug, National Research and Innovation Agency (BRIN), Cibinong, Bogor, Jawa Barat, 16911, Indonesia*

(Received March 23, 2022; Revised May 27, 2022; Accepted June 04, 2022)

Abstract: Type 2 diabetes mellitus is a disease caused by insulin resistance. Many types of oral medications exist, but the effectiveness and side effects differ from patient to patient, so alternative drugs are still required. One compound group receiving much scientific interest regarding its antidiabetic potential is xanthones as potential alpha-glucosidase and alpha-amylase inhibitors. This study performed molecular docking simulations on all 515 natural xanthones with alpha-glucosidase and alpha-amylase as the protein targets. We found 31 unique ligands that comply, and the three best ligands per protein target were filtered based on how many active site residues the ligands interacted with the targets. The three best alpha-glucosidase inhibitors are 3,4,5,8-tetrahydroxy-1,2-diisoprenylxanthone, Polygalaxanthone V, and Polygalaxanthone VII. As for alpha-amylase, we found 1-O-primeverosyl-3,8-dihydroxy-5-methoxyxanthone, Garcimangosone C, and Mangostinone as the best inhibitors. The six chosen and standard ligands underwent 2 ns molecular dynamics simulations. Both standard ligands had the highest interaction energies, followed by complexes with glycosylated xanthones, and prenylated xanthones. We also found that the prenylated xanthones could retain their initial protein-ligand interactions. Therefore, this is the first study that revealed prenylated xanthones have a good potential as anti-type 2 diabetes mellitus agents among other xanthones groups through in silico method.

Keywords: Molecular docking; molecular dynamics; xanthone, alpha-amylase inhibitor; alpha-glucosidase inhibitor. © 2022 ACG Publications. All rights reserved.

1. Introduction

Type 2 diabetes mellitus (T2DM) is a disease caused by the body's resistance to insulin, which could result in hyperglycemic conditions (high blood glucose levels), leading to organ failure or destruction [1]. A variety of T2DM oral medications exist including oral drugs. Most oral antidiabetic drugs in the market fall into one of six categories: biguanides, sulphonylureas, glinides,

* Corresponding author: E-Mail: mmiftahjauhar@nano.or.id; Phone: +6281-391-674703 *Fax*: +6281-391-674703

The article was published by ACG Publications
http://www.acgpubs.org/journal/records-of-natural-products January-February 2023 EISSN:1307-6167
DOI: http://doi.org/10.25135/rnp.337.2203.2391
Available online: June 21, 2022

thiazolidinediones, and dipeptidylptidase IV (DPP-IV) inhibitors, and alpha-glucosidase inhibitors [2]. Though many oral medications have been developed, treatment effectiveness and side effects are variable among patients [3,4]. Due to these reasons, alternative drug candidates are still required.

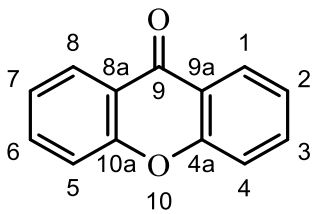

Figure 1. Xanthone's general structure

One group of compounds that have garnered interest in its antidiabetic activities is xanthones, especially the xanthones' roles as alpha-glucosidase and alpha-amylase inhibiting agents. Xanthones are one metabolite family group that can be found in various plants, particularly Clusiaceae and Gentianaceae families. Its basic skeleton is built by conjugated ring composed of aromatic ring with carbonyl group and oxygen atom (Figure 1) [5]. Furthermore, alpha-glucosidase and alpha-amylase are two proteins that play a part in complex-carbohydrate metabolism. Inhibition of these enzymes decreases carbohydrate degradation into glucose, slowing down the increase of blood glucose concentration [6,7].

515 natural xanthones were reported in the literature [8]. Although plenty of research have been performed on certain xanthones as antidiabetic candidates [9-14], at present, no research has attempted to compare the ability of all 515 natural xanthones to inhibit these two enzymes. Bairy *et al* showed that as many as 28 types of xanthone have a good ability as an inhibitor of alpha-glucosidase using in silico method [15]. Furthermore, Malik *et al* revealed an inhibitor potential of alpha-glucosidase from *Penicillium canescens* as xanthones' source [4]. This research aims to investigate the potential of 515 xanthones as alpha-glucosidase and alpha-amylase inhibitors using in silico approaches: molecular docking and molecular dynamics. Molecular docking was performed on the two protein targets mentioned before. These two enzymes are direct targets of acarbose, a commonly used T2DM drug in the alpha-glucosidase inhibitor class [16]. Alpha-glucosidase is represented by protein 2QMJ [17], which is complex with acarbose, while alpha-amylase is represented by protein 1XD0 [18], which is complex with acarbose-αG3F. These two molecules act on the controls for each protein target in the molecular docking and molecular dynamics simulations.

2. Materials and Methods

2.1. Ligand and Structure Preparations

Reference [8] provides a list of 515 known natural xanthones (Table S3). According to the list, the three-dimensional structures were either downloaded in its structure data file (.sdf) format (if available on Pubchem) or created using Avogadro and saved as .mol2 files. SMILES strings were also collected as the input for ADME and toxicity estimation simulations. In addition, 3D structures of the two protein targets, 2QMJ and 1XD0, were gathered from an online protein data bank of RCSB PDB.

2.2. ADME-Tox Predictions

ADME simulations were carried out by using SwissADME, which receives compound structures in SMILES strings as input and outputs predicted physicochemical values [19]. In this case, the string input was made of SMILES of each xanthone derivative. The results of the ADME predictions were used as complementary information for finding which ligands ranked at the top according to the docking results. Afterward, toxicity estimation was done with the help of T.E.S.T

5.1.1 software to make sure the chosen xanthones do not have very high toxicity levels [20]. The parameter for this estimation was oral rat LD50 in mg/kg.

2.3. Molecular Docking

Molecular docking was performed using PyRx 0.8 [21]. Before beginning the simulation, CHARMM forcefield and MMFF94 partial charge were applied to each xanthone's three-dimensional structure file. These xanthones acted as ligands while the two proteins acted as macromolecules. The search spaces and dimensions for proteins 2QMJ and 1XD0 respectively were (8.224, 14.808, 50.737; 30.938 × 26.053 × 29.224) and (−18.797, −3.176, −14.225; 34.647 × 34.832 × 34.626).

2.4. Conserved Amino Acid Analysis

2QMJ and 1XD0 Fasta were collected from the NCBI website. Protein Basic Local Alignment Search Tool (BLAST-P) was conducted to search the top ten similar protein sequences of 2QMJ and 1XD0. The top ten sequences were retrieved and analyzed for their similarity to 2QMJ and 1XD0 protein using the Clustal Omega web server. Output format was ClustalW with character counts and the rest parameters were default.

2.5. Molecular Dynamics

Molecular dynamics simulations were performed using GROMACS 5.1.1 with CHARMM forcefield (February 2021 version) and TIP3P water model [22]. Ligand topology was created on the CGenFF website. Before the production step, energy minimization was performed using the steepest descent algorithm, and equilibration was done using the NVT and NPT ensembles at 310K and 1 atm with a simulation time of 100 ps. Once energy minimization and equilibration were successful, the experiment carried on to the production step at 2 ns.

3. Results and Discussion

3.1. Ligand and Protein Structure Preparations

Xanthones as a natural product have the potential to be an alternative inhibitor of alpha-glucosidase and alpha-amylase. Its ability to inhibit these targets is structurally dependent, especially on the presence of hydroxyl group, hydrogen bonding, and other molecular interactions such as π-π stacking [23,24]. To develop a potential drug for inhibiting protein receptor some parameters is important to be considered such as drug-likeness and stabilization of inhibition ability of the drug to its target [25,26]

Table 1 provided information on how many xanthones in each group do not adhere to Lipinski's rule of five (Ro5). It was found that 81.7% of xanthones fulfill all Lipinski rules, suggesting that most xanthones have similar physicochemical characteristics to oral drugs. From the xanthone groups, 100% of simple xanthones and 91.2% of prenylated xanthones have high drug-likeness as these xanthones comply with all four of Lipinski's Ro5. On the other hand, very few glycosylated xanthones and bis-xanthones follow the Ro5, while the general drug-likeness of xanthonolignoids and miscellaneous xanthones could not be concluded as there are very few compounds in said xanthone groups.

Table 2 shows the results of toxicity estimation of the xanthone compounds in terms of Oral Rat LD50. From the table, it was found that most xanthones are predicted to be slightly toxic (54.0%) or moderately toxic (31.17%). The average toxicity of xanthones was estimated to be about 814 mg/kg. Toxicity is a crucial characteristic in drug development [27]. The T.E.S.T 5.1.1 software uses physical and chemical properties to evaluate toxicity such as molecular weight (MW) and the octanol-water partition coefficient [20]. According to Jeong *et al* [28], MW can influence the toxicity level as it tends to have a more complex structure. The complex structure with the more positive charged

group can easily interact with the cell surface and damaged the cells. Besides, the octanol-water partition as another parameter toxicity relates to hydrophobicity characteristic. A high hydrophobic compound means poorly soluble in water that can bring into slow absorption, especially in the gastrointestinal tract [29]. Research from Shi *et al* [30] showed that the greater the hydrophobicity of a compound, the greater the toxicity would be. Agree with that, according to Tables 1 and 2, the simple and prenylated xanthones groups which have lower MW and octanol-water partition (Table S3) became the most abundant that fulfill the requirements as these parameters are used in Lipinski's Ro5 screening and toxicity level.

Table 1. Number of Lipinski violations in each xanthone group

Xanthone Group	Number of Lipinski Violations					Total
	0	**1**	**2**	**3**	**4**	
Simple Xanthones	148	0	0	0	0	148
Glycosylated Xanthones	8	8	17	28	0	61
Prenylated Xanthones	259	25	0	0	0	284
Xanthonolignoids	2	0	0	0	0	2
Bis-Xanthones	0	1	5	6	0	12
Miscellaneous	4	0	2	2	0	8
Total	**421**	**34**	**24**	**36**	**0**	**515**

Table 2. Toxicity of xanthone compounds

Type of Xanthone	Number of Xanthone compound
Highly Toxic (≤ 50 mg/kg)	25
Moderately Toxic (> 50 mg/kg, ≤ 500 mg/kg)	163
Slightly Toxic (> 500 mg/kg, ≤ 5000 mg/kg)	278
Non-Toxic (> 5000 mg/kg)	0
Estimation cannot be done	49
Total	**515**

3.2. Molecular Docking Analysis

Table 3. Ligand-protein interactions with 2QMJ based on molecular docking results*

Ligand Code	Group	Toxicity (mg/kg)	Affinity (kcal/mol)	Interactions
17	Prenylated	642	−8,5	Hydrogen Bonds: **Arg526 (2)** Van der Waals: **Asp203, Met444,** Trp539 Others: **Tyr299, Asp443,** Lys480, **Asp542 (2)**, **Phe 575**
39	Prenylated	1350	−8,6	Hydrogen Bonds: Arg202 Van der Waals: Thr204, **Asp327, Phe450** Others: **Asp203, Tyr299, Ile328, Trp406, Met444,** Leu473, **Arg526, Asp542**, Phe575
55	Prenylated	681	−8,6	Hydrogen Bonds: Arg202, Thr205 (2) Van der Waals: Asn207, **Arg526, Asp542** Others: **Asp203,** Thr204 (2), **Tyr299,** Leu473, **Phe575**
76	Prenylated	672	−8,5	Hydrogen Bonds: **Phe450** Van der Waals: **Asp327, Ile328, Asp542** Others: **Ile364**, **Trp406, Trp441, Phe450 (3**), **Phe575, His600**

Ligand Code	Group	Toxicity (mg/kg)	Affinity (kcal/mol)	Interactions
115	Glycosylated	2887	−8,7	Hydrogen Bonds: Arg202 (2), Thr205, **Tyr299, Asp443, Arg526, Asp542 (2)** Van der Waals: **Asp203, Met444,** Asn449, Asp474, Trp539, **Phe575** Others: Arg202, Thr204 (2), Thr205, Leu473, Lys480
117	Glycosylated	2049	−8,8	Hydrogen Bonds: **Asp203 (2), Asp327, Asp443, Arg526, Asp600,** Gln603 (2) Van der Waals: Arg202, **Trp441, Met444,** Ser448, **Phe450,** Trp539, Gly602, **Tyr605** Others: **Tyr299, Trp406 (2), Asp542, Phe575,** Ala576
119	Glycosylated	1838	−8,8	Hydrogen Bonds: **Asp203, Asp443, Arg526** Van der Waals: **Met444,** Ser448, **Phe450,** Trp539, Gly602, Gln603, **Tyr605** Others: Arg202, **Tyr299, Trp406 (2), Asp542 (2), Phe575**, Ala576
140	Prenylated	1699	−9,1	Hydrogen Bonds: **Asp203**, **Arg526** Van der Waals: **Asp327, Trp441, Asp443, Met444,** Ser448, **Phe450,** Gly602, Gln603 Others: **Tyr299 (3), Ile328, Ile364, Trp406 (4), Asp542, Phe575 (2), Tyr605**
267	Prenylated	962	−8,9	Hydrogen Bonds: **Asp203, Arg526** Van der Waals: **Asp327, Trp441, Asp443, Met444,** Ser448, Trp539, Gly602, Gln603 Others: **Tyr299, Trp406 (2), Phe450 (2), Asp542 (2)**, **Phe575, His600, Tyr605**
384	Prenylated	822	−8,5	Hydrogen Bonds: **Asp203, Arg526** Van der Waals: **Met444,** Ser448, Trp539, Gly602, Gln603 Others: **Tyr299, Trp406 (2), Asp443, Phe450, Asp542 (2), Phe575, Tyr605**
400	Glycosylated	2250	−8,8	Hydrogen Bonds: **Asp203, Asp327,** Glu404, Lys480, **Arg526** Van der Waals: Thr204, **Asp443, Met444,** Ser448, Trp539, **His600** Others: Arg202, **Tyr299**, **Trp406 (2), Phe450, Asp542 (2), Phe575**
424	Glycosylated	2793	−9	Hydrogen Bonds: **Asp203, Asp327, Phe450, Asp542 (3), His600** Van der Waals: **Trp406, Trp441, Arg526, Phe575** Others: **Asp203, Phe450 (3)**
448	Glycosylated	1432	−8,7	Hydrogen Bonds: **Asp203, Tyr299, Asp327, Arg526 (2), Asp542, His600,** Gln603 Van der Waals: **Ile328, Ile364, Asp443,** Ser448, **Phe575** Others: **Tyr299, Trp441,** Trp539, Ala576 (2)

Ligand Code	Group	Toxicity (mg/kg)	Affinity (kcal/mol)	Interactions
449	Glycosylated	2272	−8,7	Hydrogen Bonds: **Trp406, Arg526, Asp542, His600,** Gln603 Van der Waals: **Asp203, Asp327, Ile328, Ile364, Asp443, Met444, Phe450, Phe575** Others: **Tyr299, Trp441,** Ala576 (2), Trp539, **His600**
451	Glycosylated	2598	−8,5	Hydrogen Bonds: **Trp406, Asp443, Arg526, Asp542**, Gln603 Van der Waals: **Asp203, Asp327, Ile328, Ile364, Met444**, **Phe450, Phe575** Others: **Tyr299, Trp441,** Trp539, Ala576 (2), Leu577, **His600**
510	Glycosylated	1137	−8,6	Hydrogen Bonds: **Asp203 (2),** Ser448, Asn449, **Arg526, Asp542** Van der Waals: Thr204, **Met444, Phe450,** Lys480, Trp539 Others: Arg202, **Tyr299, Trp406 (2), Asp443, Asp542 (2), Phe575**
Control			−7,8	Active site: **His600, Asp327, Asp203, Arg526, Asp542, Met444, Tyr605, Asp571** (Hydrogen bond) **Ile328, Ile364, Trp441, Tyr229, Asp443, Trp406, Phe450, Phe575** (Van der waals)

*Interactions at the target's active site residues based on the reference are marked in red.

Table 4. Ligand-Protein Interactions with 1XD0 Based on Molecular Docking Results*

Ligand Code	Group	Toxicity (mg/kg)	Affinity (kcal/mol)	Interactions
L17	Prenylated	642	−10,9	Hydrogen Bonds: **Asp197,** Ala198 Van der Waals: **His101**, Thr163, Leu165, Ser199, Val234, His299, His305 Others: Leu162 (2), Ala198 (2), **Lys200 (2), His201 (2)**, **Glu233,** Ile235, **Asp300**
L55	Prenylated	681	−9,8	Hydrogen Bonds: **Glu233** Van der Waals: Trp58, Thr163, Ala198, Ser199, Val234, His305 Others: Trp59 (2), Tyr62, Ile162 (2), Leu165 **(2), Lys200, His201**, Ile235, **Asp300**
L76	Prenylated	672	−9,9	Hydrogen Bonds: Lys200, **Glu233, Glu240** Van der Waals: Trp58, **His101**, Leu165, Ala198 Others: Trp59, Tyr62, **Tyr151,** Leu162, **His201, Glu233,** Ile235 (2), **Asp300,** His305
L115	Glycosylated	2887	−9,7	Hydrogen Bonds: **Asp197 (2), Lys200 (2), Glu233 (2), Asp300** Van der Waals: **His101**, Leu162, **Arg195**, Ser199, Val234, **Glu240**, His299, His305, Ala307 Others: Tyr151 (2), Ala198, **Lys200, His201 (2)**, **Glu233,** Ile235 (3)

Ligand Code	Group	Toxicity (mg/kg)	Affinity (kcal/mol)	Interactions
L177	Prenylated	626	−10,4	Hydrogen Bonds: **Asp197,** Ala198, **Glu233,** Il235 Van der Waals: **His101**, Thr163, Leu165, Ser199, Val234, His299, His305 Others: Leu163 (2), Ala198, **Lys200, His201 (2), Glu233,** Ile235, **Asp300**
L209	Prenylated	914	−9,6	Hydrogen Bonds: **Glu233,** Ile235 Van der Waals: Trp59, **His101**, Thr163, Leu165, Ser199, Val234, **Glu240** Others: Tyr62, **Tyr151,** Leu162 (2), Ala198 (2), **Lys200, His201 (2), Glu233**, Ile235
L210	Prenylated	793	−9,6	Hydrogen Bonds: - Van der Waals: **His101**, Thr163, Leu165, Ala198, **Glu233,** Val234 Others: Trp58, Trp59, Tyr62, Leu162 (2), **Lys200, His201 (2)**, Ile235, His305
L241	Xanthono-lignoids	1320	−9,6	Hydrogen Bonds: **Gln63, Glu233,** Ile235 Van der Waals: Glu60, **His101**, Thr163, Ala198, Ser199, Val234 Others: Leu162 (2), Leu165 (2), **Lys200 (2), His201 (2)**, Ile235
L242	Prenylated	1032	−10	Hydrogen Bonds: - Van der Waals: Thr163, Leu165, **Lys200, Glu233** Others: **Tyr151,** Leu162 (3), Ala198 (2), **His201 (2)**, Ile235 (2), Ala307
L316	Prenylated	709	−9,8	Hydrogen Bonds: **Asp197, Glu233,** Gly306 Van der Waals: Trp58, Tyr62, Leu165, **Arg195,** Ala198, **Lys200, His299**, His305, Ala307 Others: Trp59, Tyr151, Leu162, **His201, Glu233,** Ile235, **Asp300**
L321	Prenylated	1032	−9,7	Hydrogen Bonds: **Glu233** Van der Waals: **His101**, Thr163, Leu165, Ala198, **Lys200**, His305 Others: Trp58, Tyr62, **Tyr151 (2),** Leu162 (2), **His201**, Ile235 (2), **His299**, **Asp300**
L323	Prenylated	929	−10,3	Hydrogen Bonds: **Tyr151, Asp197, Lys200** Van der Waals: **His101**, Thr163, Leu165, **Arg195, Glu233,** Val234, **Glu240** Others: **Tyr151,** Leu162 (2), **His201 (2)**, Ile235 (2), Ala198 (2), Ala307
L343	Prenylated	893	−10,6	Hydrogen Bonds: - Van der Waals: Trp58, Tyr62, **His101**, Thr163, Leu165, **Arg195**, His305 Others: Trp59 (2), Leu162 (2), Ala198 (2), Ile235, **Lys200, His201 (2), Glu233, Asp300**
L351	Prenylated	536	−9,8	Hydrogen Bonds: **Glu233** Van der Waals: Trp59, **His101,** Thr163, Leu165, **Arg195**, Ala198 Others: Tyr62, Ley162 (3), **Lys200, His201 (2)**, Ile235

Ligand Code	Group	Toxicity (mg/kg)	Affinity (kcal/mol)	Interactions
L363	Glycosylated	2512	−10,1	Hydrogen Bonds: Tyr62, **Gln63,** Thr163, **Arg195, Asp197, Lys200, Glu233, Asp300,** His305 Van der Waals: Trp58, Trp59, Leu165, Ala198, Ser199, Val234, **His299** Others: Leu162 (2), **Lys200, His201 (2),** Ile235 (2)
L372	Xanthono-lignoids	1083	−9,7	Hydrogen Bonds: Trp59, **His101, Asp197** Van der Waals: Tyr62, Thr163, Ala198, **Glu233,** Val234 Others: Leu162 (2), Leu165 (2), **Lys200, His201 (2)**, Ile235 (2)
L393	Prenylated	650	−9,8	Hydrogen Bonds: **His101, Asp197, Asp300,** His305 Van der Waals: Trp58, Val98, Leu162, Leu165, Ala198, **Glu233, His299** Others: Trp59 (2), Tyr62, Tyr151, **Lys200, His201,** Ile235
L394	Prenylated	957	−9,7	Hydrogen Bonds: **Glu233** Van der Waals: Thr163, Leu165, Ala198, Leu237, **Glu240** Others: Leu162 (2), **Lys200, His201 (2)**, Ile235 (2), **Asp300,** Ala307
L412	Prenylated	910	−10	Hydrogen Bonds: - Van der Waals: Thr163, Leu165, Ala198, **Glu233**, Val234, **Glu240**, His305 Others: **Tyr151,** Leu162 (2), **Lys200, His201 (2)**, Ile235 (2), **Asp300,** Ala307
L414	Prenylated	1589	−9,7	Hydrogen Bonds: **Glu233** Van der Waals: Leu165, Ala198, Ser199, Val234, **Glu240**, His305 Others: **Tyr151,** Leu162 (2), **Lys200, His201 (2), Glu233,** Ile235 (2), **Asp300,** Ala307
Control			−8,1	Active site: **Gln63, Thr163, Trp59, Asp197, Glu240, Lys200, His201, Glu233, Arg195, Asp300, His299, His305** (Hydrogen bond) **His101** (Van der waals)

*Interactions at the target's active site residues based on the reference are marked in red

Molecular docking of control compounds to 2QMJ and 1XD0 results in binding affinities of −7.8 kcal/mol and −8.1 kcal/mol (Tables 3 and 4), respectively. Out of the 515 xanthones, 187 had a higher affinity with protein 2QMJ, and 332 had a higher binding affinity with protein 1XD0 than the control compounds. As compounds with higher binding affinities are desired, the binding affinity cut-off was decided to be the tenth percentile of each docking simulation, which is −8.4 kcal/mol for protein 2QMJ and −9.6 kcal/mol for protein 1XD0.

Xanthones with binding affinities equal to or higher than the cut-off binding affinity and estimated to be slightly toxic at most (Oral Rat LD50 > 500 mg/kg) had their ligand-protein interactions analyzed. For proteins 2QMJ and 1XD0, 16 and 20 ligands fulfilled these conditions, respectively, as shown in Tables 3 and 4. In total, 31 unique ligands fit the cut-off points. Of the 31 ligands, 19 were prenylated xanthones, 10 were glycosylated xanthones, and the remaining two were xanthonolignoids.

3.3. Selection of Ligands

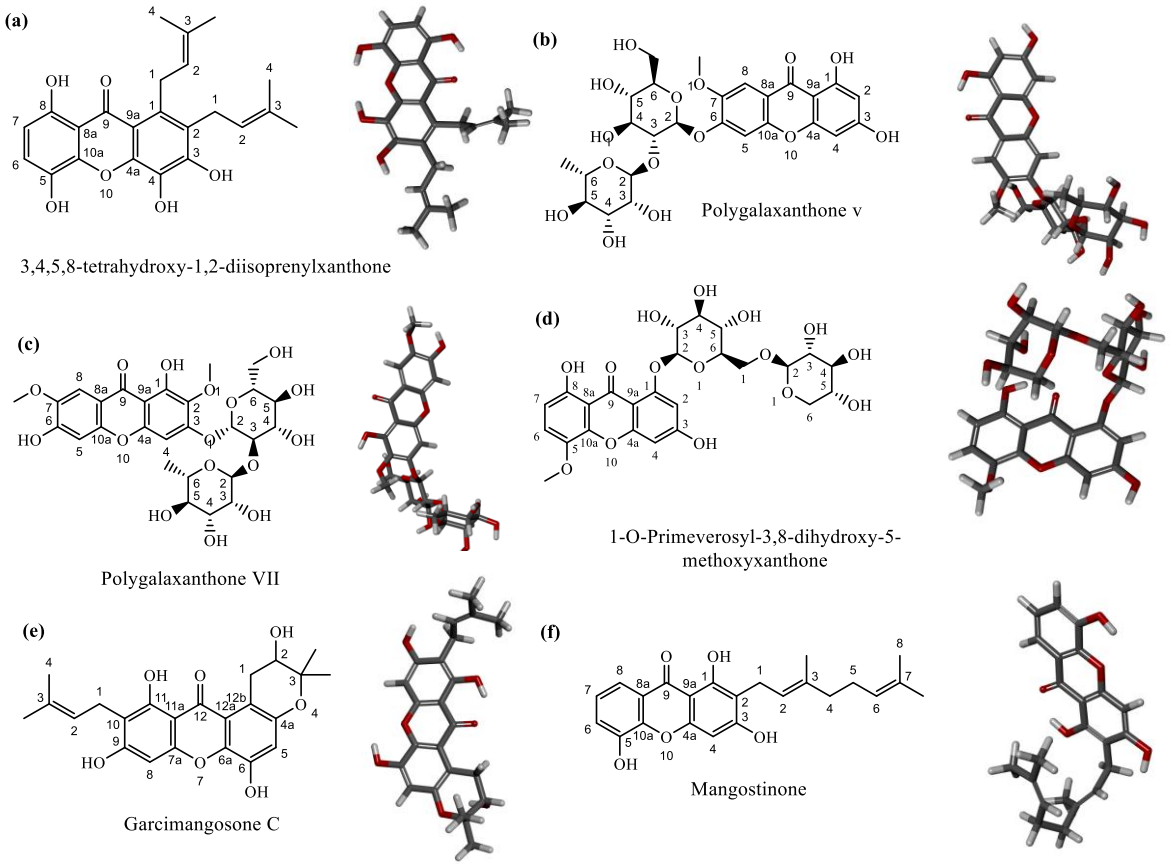

Figure 2. 2D and 3D structure of three best ligands for each protein target. (a) L140, (b) L449, and (c) L451 for 2QMJ protein. (d) L115, (e) L316, and (f) L393 for 1XD0 protein

The three best ligands for each protein target were chosen based on the number of interactions with the targets' active site residues that showed by the ligand interaction with each protein (Table 3 and 4) [12,13]. The three best ligands for 2QMJ were L140 (3,4,5,8-Tetrahydroxy-1,2-diisoprenylxanthone), L449 (Polygalaxanthone V), and L451 (Polygalaxanthone VII), while the three best ligands for 1XD0 were L115 (1-O-primeverosyl-3,8-dihydroxy-5-methoxyxanthone), L316 (Garcimangosone C), and L393 (Mangostinone).

3.3.1. L140 ligand for 2QMJ

L140 is a prenylated xanthone. It has six hydrogen acceptors and four hydrogen donors, which means that L140 does not violate any Lipinski rules and is predicted to have high gastrointestinal absorption. The predicted oral rat LD50 value for L140 is 1699 mg/kg. The binding affinity of L140 and 2QMJ is −9,1 kcal/mol, the highest of all ligand-protein affinities in Table 3. Based on the predicted ligand-protein interactions, L140 (3,4,5,8-Tetrahydroxy-1,2-diisoprenylxanthone) can interact with almost 100% of the protein's active site residues of 2QMJ that interact with the control ligand (Table 3 and Figure S1).

3.3.2. L449 Ligand for 2QMJ

L449 (Polygalaxanthone V) is a glycosylated xanthone. The ligand contains fifteen hydrogen acceptors and eight hydrogen donors, thus violating three out of four Lipinski rules, and is predicted to have low gastrointestinal absorption. The ligand is classified as slightly toxic, at 2272 mg/kg. Its

binding affinity to 2QMJ is −8,7 kcal/mol and it interacts with almost 100% of the protein's active site residues of 2QMJ that interact with the control ligand (Table 3 and Figure S2).

3.3.3. L451 Ligand for 2QMJ

L451 (Polygalaxanthone V) is a glycosylated xanthone. It has sixteen hydrogen acceptors and eight hydrogen donors, and its toxicity is 2598 mg/kg. Its binding affinity to 2QMJ is −8,5 kcal/mol. Based on molecular docking data, L451 interacts with almost 100% of the active site residues of 2QMJ of 2QMJ that interact with the control ligand (Table 3 and Figure S3).

3.3.4. L115 Ligand for 1XD0

L115 (1-O-primeverosyl-3,8-dihydroxy-5-methoxyxanthone) is a glycosylated xanthone. The compound has fifteen hydrogen acceptors and eight hydrogen donors; hence predicted to have low gastrointestinal absorption. The LD50 was estimated to be around 2887 mg/kg. The affinity of L115 with 1XD0 is −9.7 kcal/mol. It was predicted to interact with ten active site residues of 1XD0, three of them being conventional hydrogen bonds with the active residues (Asp197, Gly233, and Asp300) (Table 4 and Figure S4).

3.3.5. L316 Ligand for 1XD0

L316 (Garcimangosone C) is a prenylated xanthone. The ligand has seven hydrogen acceptors and four hydrogen donors. L316 does not violate any Lipinski rules, is predicted to have high gastrointestinal absorption, and its toxicity estimation is 709 mg/kg. Its binding affinity with 1XD0 is −9.8 kcal/mol. It interacted with eight active-site residues of 1XD0 that interact with the control ligand and would form conventional hydrogen bonds with Asp197 and Glu233 as active-site residues of 1XD0 (Table 4 and Figure S5).

3.3.6. L393 Ligand for 1XD0

L393 (Mangostinone) is a prenylated xanthone. It has five hydrogen acceptors and three hydrogen donors. The ligand's estimated toxicity was 650 mg/kg and the ligand's affinity with 1XD0 is −9.8 kcal/mol. Molecular docking results showed that L393 interacts with seven of the active site residues of 1XD0 that interact with the control ligand. It formed conventional hydrogen bonds with Asp197 and Asp300 as the active-site residue of the protein (Table 4 and Figure S6).

Based on molecular docking data, the top three ligands from each protein had higher binding affinity than the native ligand. In the molecular interaction after finishing the process, acarbose and acarbose αG3F as control ligands only had hydrogen and van der waals interaction with its receptor (Figures S7 and S8). According to the Trot and Olson [31] research, Vina molecular docking software uses some parameters to develop scoring functions such as hydrophobic interaction between hydrophobic atoms and hydrogen bonding which is a value between 1 and 0 based on distance within the interaction. Regarding the parameter, the native ligand of each protein did not build any hydrophobic interactions with its receptor (Figures S7 and S8). In contrast, three potential ligands of each protein built more than one hydrogen and hydrophobic interaction. It could be a possible cause that made the binding affinity of each native ligand lower than the others. Furthermore, Freitas *et al* [32] also stated that hydrophobic interaction is important to develop a highly efficient ligand to stabilize its receptor. Therefore, three potential ligands were considered better for their stability to the receptor than the native ligand.

Analyzing the interaction among all potential ligands and their receptor (Figures S1-S6), some amino acids that existed in all interactions with each protein were considered. These amino acids played an important role in the protein-ligand interaction as key residues. Amitai *et al* [33] and Buyong *et al* [34] showed that key residue is well-conserved in the protein sequence compared to other organisms that have high protein similarity. It is also involved in the drug development mechanism as the main active site. According to Sim *et al* [17], the main residues involved in the

catalytic site of 2QMJ protein were Tyr299, Ile328, and Ile364. The three best ligands for 2QMJ protein showed their interaction with these residues. The residues are located in the center of the substrate bind and are suggested might be responsible for the inhibitor development [17]. L140 built hydrophobic interaction with them. Aliphatic carbon from L140 interacts with aromatic carbon from Tyr299, Ile 328, and Ile364 residues of the 2QMJ protein (Figure S1). Meanwhile, L449 and L451 built hydrophobic interaction with Tyr299 using their methoxy group to the aromatic carbon of 2QMJ protein. In addition, Ile 328 and Ile 364 residues existed in both L449 and L451 as van der waals interaction (Figures S2 and S3). Furthermore, Tyr299, Ile 328, and Ile 364 were highly conserved as it was shown in Figure S9.

In the 1XD0 protein receptor, Asp 197, Glu 233, and Asp 300 were the main residues responsible for the catalytic site. The hydrogen bond that is directly bound to these residues can form a structural base for an inhibitor for this protein [18]. According to the ligand interaction of L115, L316, and L393, all of them built hydrogen bonds to these residues (Figure S4-S6). The ligand of L115 built hydrogen bonds to Glu 233 and Asp 197 using oxygen atoms from the hydroxyl group on its backbone. In addition, Asp 300 interacted using a weak hydrogen bond to L115 with partial double bond from the 1XD0 structure to the carbon atom from L115 (Figure S4). Furthermore, the ligand of L316 built hydrogen bonds with Asp 197 and Glu 233 using the hydroxyl group from the ligand to the oxygen atom from the 1XD0 structure. Meanwhile, Asp 300 involved pi-anion electrostatic interaction with L316 using a partial double bond from the 1XD0 structure to the benzene ring of L316 (Figure S5). Furthermore, the ligand of L393 built hydrogen bonds with Asp 197 and Asp 300 using hydroxyl group from the ligand to the oxygen atom and partial double bond from the 1XD0 structure respectively. In addition, Glu 233 acted as van der waals interaction in the L393-1XD0 interaction (Figure S6). Lastly, these residues were also exhibited highly conserved as it was shown in Figure S10.

3.4. Molecular Dynamics Analysis

After selecting xanthones, a molecular dynamics simulation was performed to investigate the stability of the ligand-protein complexes in the neutral solvents of water and ions, a similar condition to the fluid in human bodies. The simulation begins with system equilibration, analyzed from the systems' temperature and density stability, as well as energy minimization, analyzed from the systems' potential energy trends.

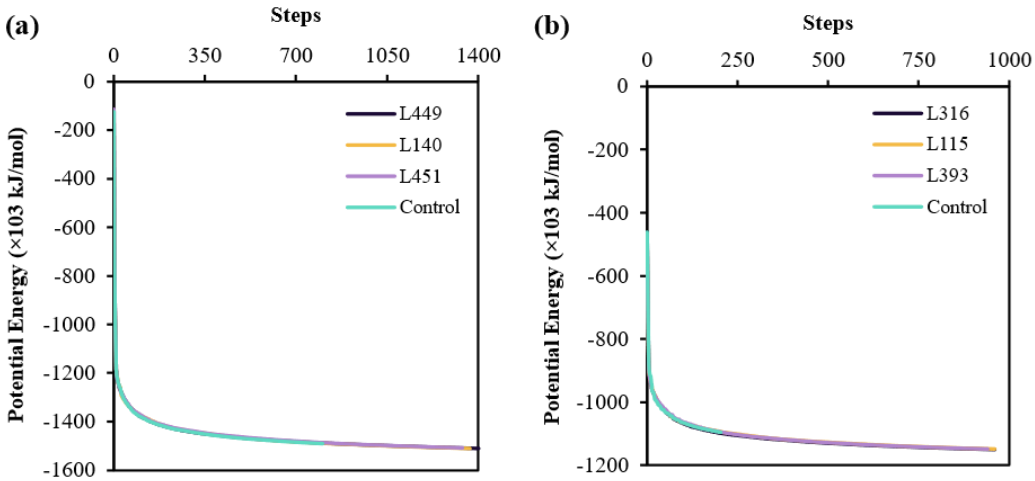

Figure 2. The potential energy of systems during energy minimization of (a) Ligands L449, L140, L451, and control on protein 2QMJ, and (b) Ligands L316, L115, L393, and control ligand on protein 1XD0

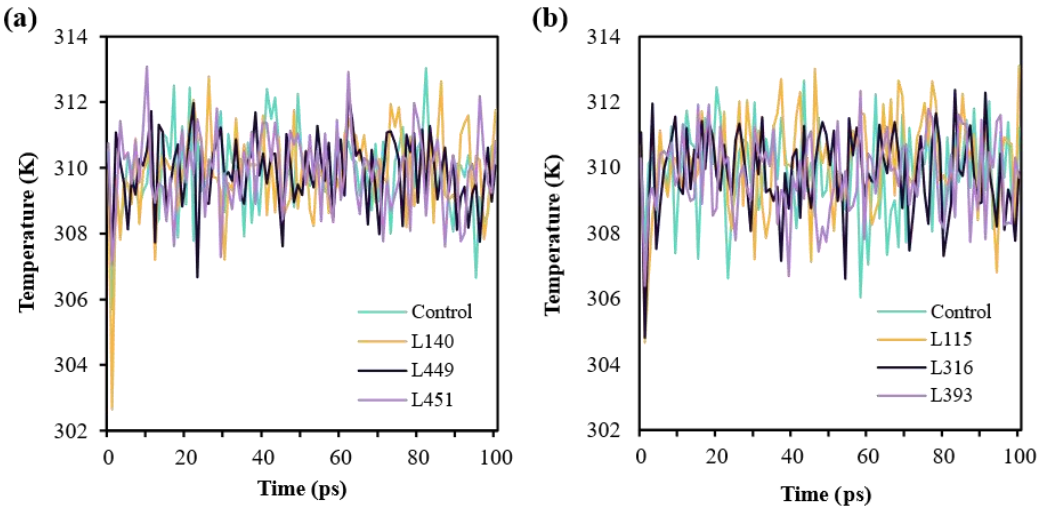

Figure 3. Temperature fluctuations of systems during equilibration of (a) Ligands L449, L140, L451, and control on protein 2QMJ, and (b) Ligands L316, L115, L393, and control ligand on protein 1XD0

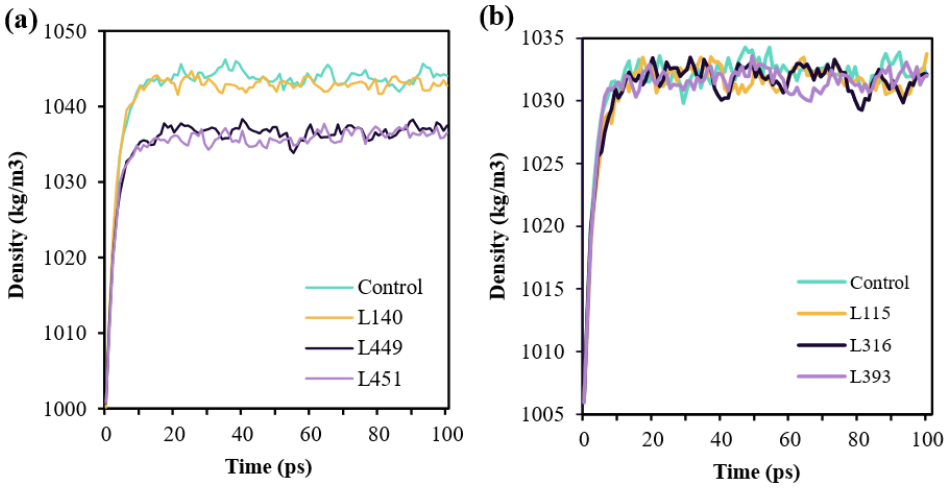

Figure 4. Density fluctuation of systems during equilibration (blue-green represents control ligand, yellow represents L140 and L115, purple represents L451 and L393, and dark blue represents L449 and L316) on proteins a) 2QMJ and b) 1XD0.

Figure 2 showed that the potential energy values became more negative and eventually stabilized over all eight systems. Therefore, the simulation was resumed to the equilibration stage. The temperature levels stabilized at 310K (Figure 3) and density levels stabilized after the simulation time of about 50 ps (Figure 4). As the equilibration process using NVT and NPT ensembles was successfully performed, the simulation was continued to the production step with the simulation time of 2 ns. From the production step results, information on each system's ligand backbone RMSD, protein residue RMSF values, and interaction energies were extracted, as shown in Figure 4, Figure 5, and Figure 6.

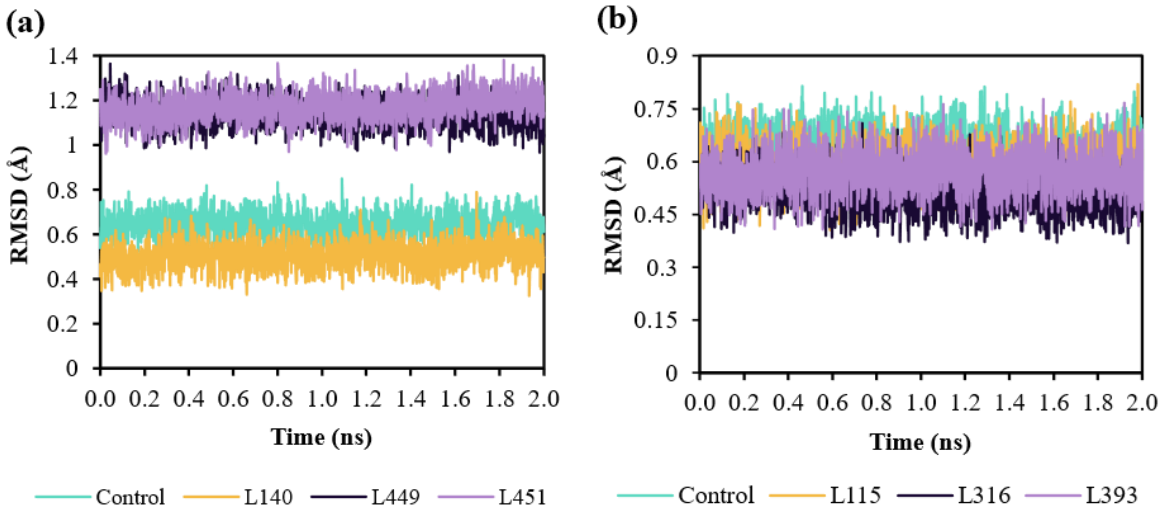

Figure 5. RMSD of ligand backbones (blue-green represents control ligand, yellow represents L140 and L115, purple represents L451 and L393, and dark blue represents L449 and L316) on proteins a) 2QMJ and b) 1XD0.

Figure 5 showed the RMSD values over time in each ligand-protein system. From the figure, it was found that all ligands had relatively stable RMSD values throughout the 2 ns simulation. In the system with protein 2QMJ, the control ligand and L140 had very low average RMSD values, respectively at 0.64 Å and 0.50 Å, while L449 and L451 had slightly higher average RMSD values of 1.14 Å and 1.17 Å. As for the ligands simulated with protein 1XD0, all four ligands (control, L115, L316, and L393) had similarly low average RMSD values of 0.64 Å, 0.59 Å, 0.51 Å, and 0.57 Å.

Figure 6 showed the hydrophobic and hydrogen interaction from each ligand during 0 ns, 1 ns, and 2 ns. Prenylated xanthones (L140, L316, and L393) built more hydrophobic interaction than glycosylated xanthones (L449, L451, and L115). Conversely, hydrogen bond interaction was more frequent in the glycosylated xanthones group than in prenylated xanthones.

In the molecular dynamics simulation, the protein-ligand complex runs in a certain period within solvent and temperature-specific aspects [35,36]. The RMSD trend represents the stability of each of these structures during their simulations. RMSD of ligands below 2 Å is considered excellent, 3 Å is acceptable, and over 3 Å is too different from its reference structure [21, 36]. From Figure 4, it was found that all ligands had relatively stable RMSD values throughout the 2 ns simulation. All eight ligands' RMSD values were still in the excellent range, which is below 2 Å, which shows that the conformation of the proteins remained accurate throughout the MD simulation.

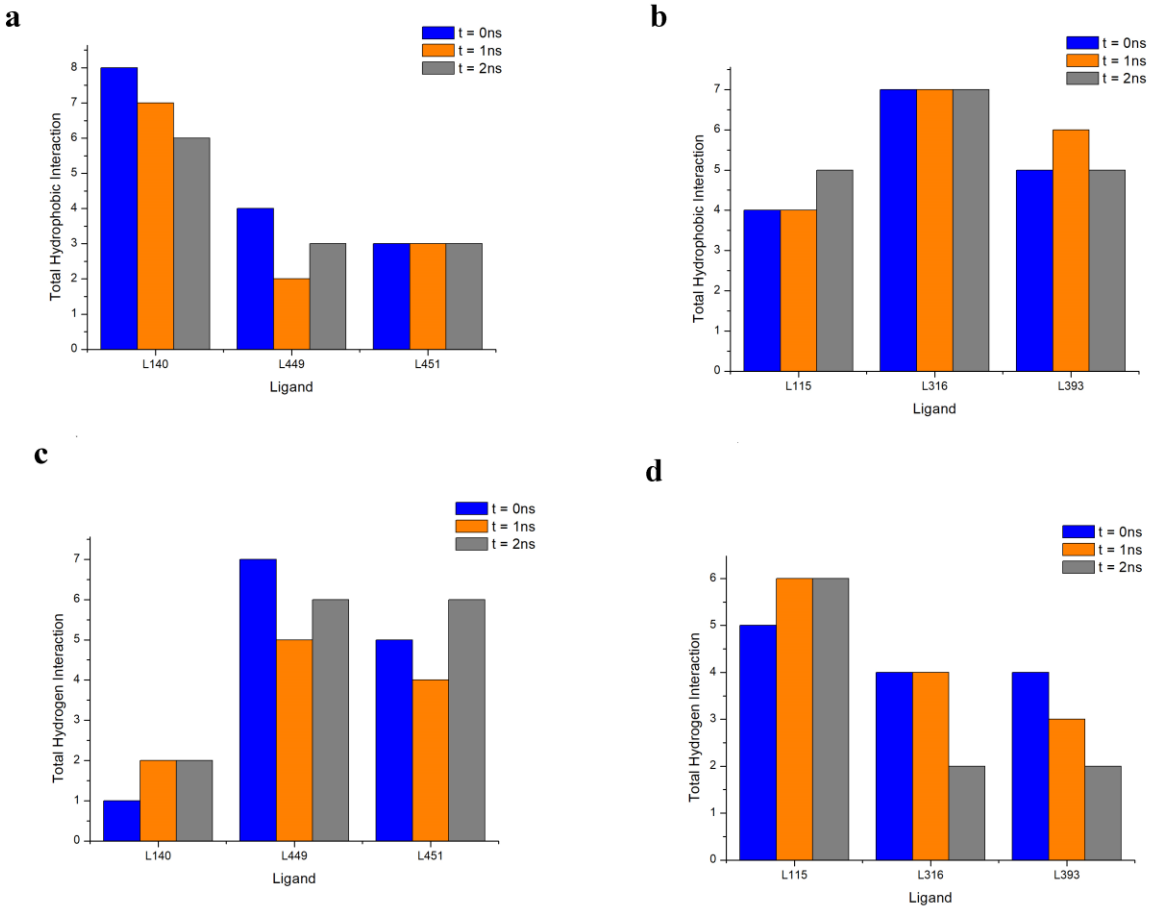

Figure 6. Hydrophobic interaction of potential ligands for (a) 2QMJ and (b) 1XD0 protein. Hydrogen interaction of potential ligands for (c) 2QMJ and (d) 1XD0 protein

In the 2QMJ protein, there were two distinct patterns of RMSD. L140 and control were around 0,6A while L449 and L451 were around 1,2 Å. The RMSD value refers to protein stabilization because of the changing in protein conformation [37]. Pace *et al* [32] showed that hydrophobic interaction majorly contributes to protein stability more than other interactions. Furthermore, conformational entropy during molecular dynamics simulation contributes to protein instability [38]. Interestingly, L140 and control had more than four amino acid residues that produced hydrophobic interaction during molecular dynamics simulation at t=0 ns, t=1 ns, and t=2 ns (Figure. 6a). In contrast, L449 and L451 only have around three residues that produce hydrophobic interaction (Figure. 6a). This could be a reason that made control and L140 had lower RMSD values. Next, in the 1XD0 protein complexes, the RMSD value tended to be more stable in all ligands around 0,6 Å. It was linear to the hydrophobic bond in these ligands that involved around four amino acid residues (Figure. 6b).

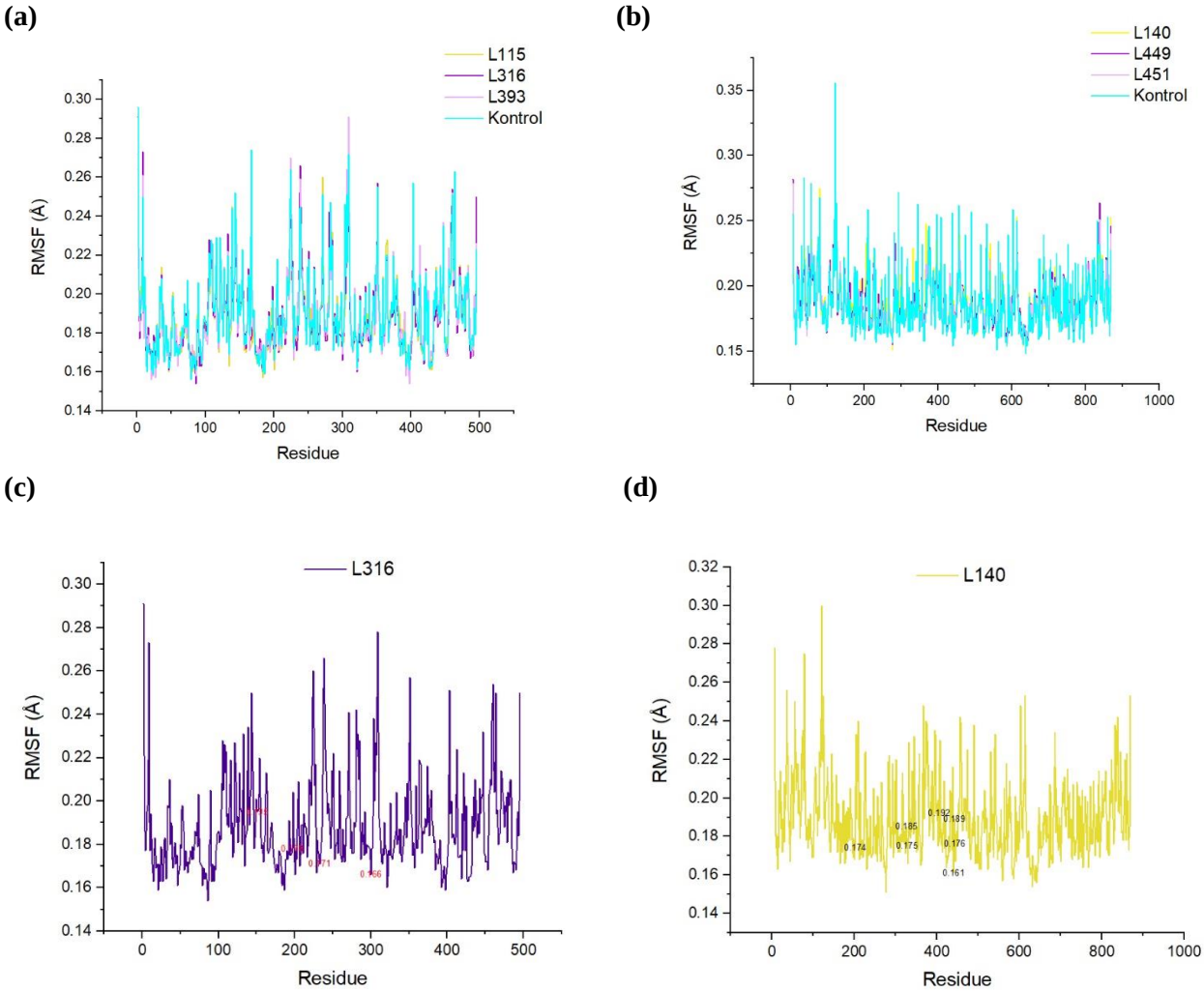

Figure 7. RMSF of residues in proteins a) all ligands in 2QMJ, b) all ligands in 1XD0 protein. Prenylated xanthones of c) L316 in 2QMJ protein and d) L140 in 1XD0 protein

Figure 7 shows the RMSF values of residues of each target protein. Root Mean Square Fluctuations (RMSF) is the average displacement of atoms or groups of atoms along with the simulation compared to its reference structure, which helps indicate the stability of these proteins' atoms or residues [39]. The residue annotations given in Figure 7 showed binding sites with lower RMSF values that suggest the binding between site residues and the ligands will be more stable.

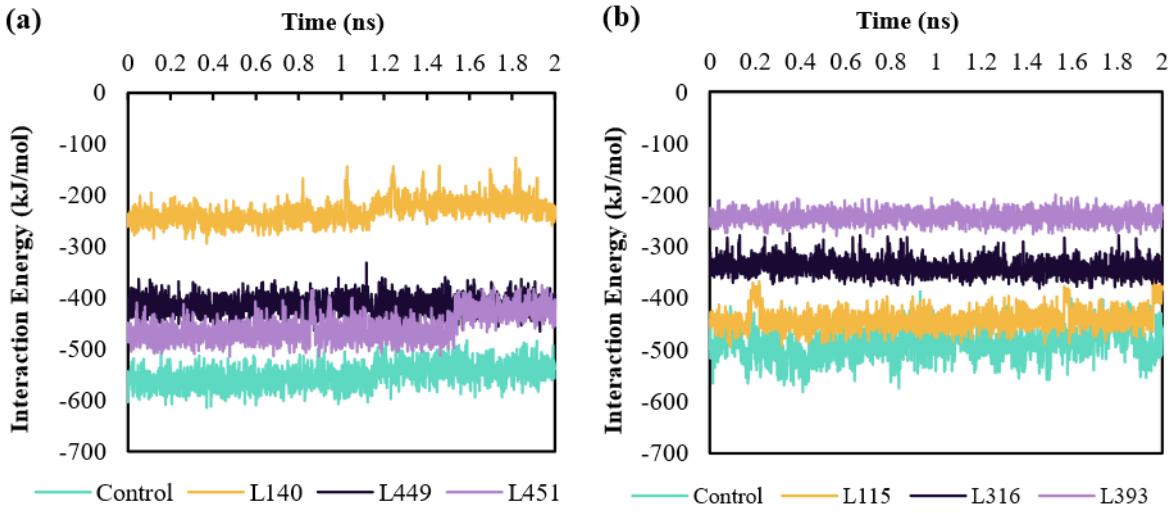

Figure 8. Interaction Energies of ligands (blue-green represents control ligand, yellow represents L140 and L115, purple represents L451 and L393, and dark blue represents L449 and L316) in proteins a) 2QMJ and b) 1XD0.

Figure 8 showed the interaction energies of ligands over time. The interaction energy levels of L140, L451 and the control ligand with protein 2QMJ experienced a gradual loss of interaction energy, while the interaction with L449 seemed relatively stable. For the interactions with protein 1XD0, L316 and L393 seemed relatively stable, L115 fluctuated slightly, and the control ligand's interaction energy decreased.

Alongside RMSD, we also evaluate RMSF on each potential ligand. According to Figure 7, all potential ligands from both proteins almost showed a similar result. Then, L316 from 2QMJ protein and L140 from 1XD0 protein were chosen as they showed low RMSD to investigate further. RMSF can exhibit each residue fluctuation in the protein structure. Based on Figure 7c and d, key residues in the active site exhibited low fluctuation than other regions. De Vita *et al* [40] stated that low fluctuation in the binding site indicates the strong binding from the ligand to its protein. Therefore, these ligands can bind strongly to the 2QMJ and 1XD0 proteins.

On the other side, according to Figure 8, the interaction energy values correlated with the chemical subgroup family of each ligand. The control ligands had the highest interaction energy in both systems, followed by glycosylated xanthones (L449, L451, and L115), and lastly, the prenylated xanthones (L140, L316, and L393). This could have occurred because of the hydrogen bonding existing in the protein-ligand interaction. A hydrogen bond is considered a moderate interaction level according to the binding energy after covalent interaction and higher than the other interactions such as electrostatic and van der waals bonding [41]. According to the ligand-protein interaction in Figure 6, glycosylated xanthones and prenylated xanthones groups had a different quantity of hydrogen interaction. Glycosylated xanthones have six amino acids that build hydrogen bonding during molecular dynamic simulation, in contrast, prenylated xanthones were only built around three amino acids (Figures 6c and 6d). Thangapandian *et al* [42] showed that the ligand-complex that did not build any hydrogen bonds tended to have higher energy during the molecular dynamic simulation and it can influence the affinity ability of the ligand to its receptor. However, Freitas *et al* [32] revealed that hydrophobic interaction became the most prominent in the high-efficiency protein-ligand complex after analyzing around 6000 protein-ligand complexes in the PDBBind database. This finding was related to the characteristic of a binding pocket that was more hydrophobic. Furthermore, optimization using hydrophobic interaction is less challenging than increasing the hydrogen bond itself [31]. Regarding these, it was linear to the molecular dynamics result of glycosylated xanthones and prenylated xanthones group. Glycosylated xanthones tended to have lower interaction energy while their RMSD was higher fluctuation. In contrast, prenylated xanthones showed higher interaction energy and their RMSD was lower fluctuation.

According to Table S1, L140 as prenylated xanthones kept 70% of their initial interactions and showed the highest percentage of their interactions during 2 ns for 2QMJ protein. Meanwhile, in Table S2, ligand L393 as prenylated xanthones kept 72.7% of their initial interactions and showed the highest percentage of their interactions during 2 ns for 1XD0 protein. In addition, some researchers have reported the potential of prenylated xanthones to build strong binding with protein targets. Bernal *et al* [43] evaluated 272 natural xanthones' activity to inhibit ten enzymes that are crucially involved in the metabolic process of microorganisms using molecular docking. The research found that the inhibition activities were related to the xanthone's classification especially the presence or absence of the prenyl group. Prenylated xanthones showed stronger enzyme inhibition to the tested enzymes than other groups. Furthermore, Khaw *et al* [44] revealed that prenylated xanthones from *Garcinia mangostana* extract had a good potential for cholinesterase inhibitors. All three compounds built hydrophobic interaction to the binding site of the tested protein. The hydrophobic interaction mainly involved pi-pi interaction using the structural benzene ring of the compound. In a similar way, this research also found that hydrophobic interaction became the major contribution to build strong binding with the protein.

In conclusion, prenylated xanthones exhibited a good inhibitor for alpha-glucosidase and alpha-amylase as an anti-type 2 diabetes mellitus target. Prenylated xanthones are one of the major xanthone groups that contain around 285 compounds. It makes them the most abundant group of xanthones regarding the number isolated from the natural source. The source of this xanthones group is various in the plant since it has some derivative structures. Prenylated mono-oxygenated xanthones are commonly isolated from *Calophyllum teysmannii* var. *inophylloide*, prenylated di-oxygenated xanthones come from the family *Clusiaceae* plant, and prenylated tri-oxygenated xanthones are broad in *Clusiaceae*, Annonaceae, and Moraceae plants [7,45]. In several studies using in vitro method, prenylated xanthones were revealed as a promising therapeutic for anticancer, antibacterial, and immunomodulatory agents [46-48]. Furthermore, this is the first study to reveal that prenylated xanthones have a good potential as an anti-type 2 diabetes mellitus agent through in silico method. Further research is important to show the deeper mechanism of prenylated xanthones as therapeutic agents.

Acknowledgments

We are grateful to the Bandung Institute of Technology under Penelitian, Pengabdian Masyarakat, dan Inovasi (PPMI) Scheme and grant number of STEI.PPMI-1-16-2021 and Nano Center Indonesia for their financial support.

Supporting Information

Supporting information accompanies this paper on http://www.acgpubs.org/journal/records-of-natural-products

ORCID
Michaella Yosephine: 0000-0002-6380-9865
Isa Anshori: 0000-0001-5134-7264
Muhammad Miftah Jauhar: 0000-0002-5826-5904
Putri Hawa Syaifie: 0000-0001-8566-7960
Adzani Gaisani Arda: 0000-0002-2674-6295
Azza Hanif Harisna: 0000-0002-8313-7058
Dwi Wahyu Nugroho: 0000-0002-7020-8582
Etik Mardliyati: 0000-0002-3621-9659

References

[1] American Diabetes Association (2011). Diagnosis and classification of Diabetes Mellitus, *Diabetes Care*. **34**, (Suppl 1). S62–S69.

[2] D. M. Nathan (2007). Finding new treatments for diabetes--how many, how fast... how good?, *NEJM*. **356**, 437–440.

[3] A. Chaudhury, C. Duvoor, V. S. D. Reddy, S. Kraleti, A. Chada, R. Ravilla, A. Marco, N. S. Shekhawat, M. T. Montales, K. Kuriakose, A. Sasapu, A. Beebe, N. Patil, C. K. Musham, G. P. Lohani and W. Mirza (2017). Clinical Review of Antidiabetic Drugs: Implications for Type 2 Diabetes Mellitus Management, *Front. Endocrinol*. **8**, 6.

[4] A. Malik, H. Ardalani, S. Anam, L. M. McNair, K. J. K. Kromphardt, R. J. N. Frandsen, H. Franzyk, D. Staerk and K. T. Kongstad (2020). Antidiabetic xanthones with α-glucosidase inhibitory activities from an endophytic Penicillium canescens, *Fitoterapia* **142,**104522.

[5] K. Niaz and F. Khan (2020). Analysis of polyphenolics, *Rec. Adv. Nat. Prod. Anal*. **3**, 39-197.

[6] F. A. Van de Laar (2008). Alpha-glucosidase inhibitors in the early treatment of type 2 diabetes, *Vasc. Health. Risk. Manag*. **4**, 1189 – 1195.

[7] L. Gong, D. Feng, T. Wang, Y. Ren, Y. Liu and J. Wang (2020). Inhibitors of α-amylase and α-glucosidase: Potential linkage for whole cereal foods on prevention of hyperglycemia, *Food Sci. Nutr*. **8**, 6320–6337.

[8] L. M. Vieira and A. Kijjoa (2005). Naturally-occurring xanthones: recent developments, *Curr. Med. Chem*. **12**, 2413-2446.

[9] C. M. Santos, M. Freitas and E. Fernandes (2018). A comprehensive review on xanthone derivatives as α-glucosidase inhibitors, *Eur. J. Med. Chem*. **157**, 1460-1479.

[10] J. Wairata, A. Fadlan, A.S. Purnomo, M. Taher and T. Ersam (2021). Total phenolic and flavonoid contents, antioxidant, antidiabetic and antiplasmodial activities of *Garcinia forbesii* King: A correlation study, *Arab J. Chem*. **10**, 103541.

[11] J. Wairata, E. R. Sukandar, A. Fadlan, A. S. Purnomo, M. Taher and T. Ersam (2021). Evaluation of the antioxidant, antidiabetic, and antiplasmodial activities of xanthones isolated from garcinia forbesii and their in silico studies, *Biomedicines* **9**, 1380.

[12] T. J. Bamigboye, O. J. Idowu, O. O. Olujide and V. H. R. Fanie (2020). Structure-activity relationship of the polyphenols inhibition of α-amylase and α-glucosidase, *J. Complement Altern Med*. **17**, 55-65.

[13] G. Nag, S. Das, S. Das, S. Mandal and B. De (2015). Antioxidant, anti-acetylcholinesterase and anti-glycosidase properties of three species of Swertia, their xanthones and amarogentin: A comparative study, *Phcog J*. **7**, 117-123.

[14] O. Tusevski, M. Krstikj, J. P. Stanoeva, M. Stefova and S. Gadzovska Simic (2018). Phenolic profile and biological activity of *Hypericum perforatum* L.: can roots be considered as a new source of natural compounds?, *S. Afr. J. Bot*. **117**, 301-310.

[15] P. S. Bairy, A. Das, L. M. Nainwal, T. K. Mohanta, M. K. Kumawat, P. K. Mohapatra and P. Parida (2016). Design, synthesis and anti-diabetic activity of some novel xanthone derivatives targeting a-glucosidase, *Bangladesh J. Pharmacol*. **11**, 308 – 318.

[16] N. Etsassala, J. A. Badmus, J. L. Marnewick, E. I. Iwuoha, F. Nchu and A. A. Hussein (2020). Alpha-glucosidase and alpha-amylase inhibitory activities, molecular docking, and antioxidant capacities of *Salvia aurita* constituents, *Antioxidants*. **9**, 1149.

[17] L. Sim, R. Quezada-Calvillo, E. E. Sterchi, B. L. Nichols and D. R. Rose (2008). Human intestinal maltase-glucoamylase: crystal structure of the N-terminal catalytic subunit and basis of inhibition and substrate specificity, *J. Mol. Biol*. **375**, 782–792.

[18] C. Li, A. Begum, S. Numao, K. H. Park, S. G. Withers and G. D. Brayer (2005). Acarbose rearrangement mechanism implied by the kinetic and structural analysis of human pancreatic alpha-amylase in complex with analogues and their elongated counterparts, *Biochemistry* **44**, 3347–3357.

[19] A. Daina, O. Michielin and V. Zoete (2017). SwissADME: a free web tool to evaluate pharmacokinetics, drug-likeness and medicinal chemistry friendliness of small molecules, *Sci. Rep*. **7**, 42717.

[20] T. Martin (2016). User's Guide for T.E.S.T. (Toxicity Estimation Software Tool), *U.S. Environmental Protection Agency*. pp, 8-11.

[21] S. Dallakyan and A. J. Olson (2015). Small-molecule library screening by docking with PyRx, *Methods mol. biol*. **1263**, 243–250.

[22] J. Lemkul (2019). From proteins to perturbed hamiltonians: a suite of tutorials for the gromacs-2018 molecular simulation package, *Live. Co. MS.* **1**, 1.

[23] Y. Liu, L. Ma, W. H. Chen, B. Wang and Z. L. Xu (2007). Synthesis of xanthone derivatives with extended pi-systems as α-glucosidase inhibitors: insight into the probable binding mode, *Bioorg. Med. Chem*. **15**, 2810–2814.

[24] Y. Liu, L. Ma, W. H. Chen, H. Park, Z. Ke and B. Wang (2013). Binding mechanism and synergetic effects of xanthone derivatives as noncompetitive α-glucosidase inhibitors: a theoretical and experimental study, *J. Phys. Chem. B*. **43**, 13464–13471.

[25] A. Zerroug, S. Belaidi, I. BenBrahim, L. Sinha and S. Chtita (2019). Virtual screening in druglikeness and structure/activity relationship of pyridazine derivatives as Anti-Alzheimer drugs, *J. King Saud Univ - Sci*. **31**, 595–601.

[26] M. Nedyalkova, M. Vasighi, S. Sappati, A. Kumar, S. Madurga and V. Simeonov (2021). Inhibition ability of natural compounds on receptor-binding domain of sars-cov2: an in silico approach, *Pharmaceuticals* **14**, 1328.

[27] S. Pasuraman (2011). Toxicological screening, *J. Pharmacol. Pharmacother*. **2**, 74–79.

[28] H. Jeong, J. Hwang, H. Lee, P.T. Hammond, J. Choi and J. Hong (2017). In vitro blood cell viability profling of polymers used in molecular assembly, *Nature* **7**, 9481.

[29] K. T. Shavjani, A. K. Gajjar and J. K. Savjani (2012). Drug solubility: importance and enhancement techniques, *ISRN Pharm*. **2012**, 195727.

[30] J. Q. Shi, J. Cheng, F. Y. Wang, A. Flamm, Z. Y. Wang, X. Yang and S. X. Gao (2012). Acute toxicity and n-octanol/water partition coefficients of substituted thiophenols: determination and QSAR analysis, *Ecotoxicol. Environ. Saf*. **78**, 134-141.

[31] O. Trott and A. J. Olson (2010). AutoDock Vina: improving the speed and accuracy of docking with a new scoring function, efficient optimization, and multithreading, *J. Comput. Chem*. **31**, 455-461.

[32] R. Ferreira de Freitas and M. A. Schapira (2017). Systematic analysis of atomic protein-ligand interactions in the PDB, *MedChemComm*. **8**, 1970-1981.

[33] G. Amitai, A. Shemesh, E. Sitbon, M. Shklar, D. Netanely, I. Venger and S. Pietrokovski (2004). Network analysis of protein structures identifies functional residues, *J. Mol. Biol*. **344**, 1135–1146.

[34] M. Buyong, E. Tal, W. Haim, and N. Ruth, (2003), *Proc. Natl. Acad. Sci. U.S.A.* **100**, 5772.

[35] V. D. Prasasty, S. Cindana, F.X. Ivan, H. Zahroh and E. Sinaga (2020). Structure-based discovery of novel inhibitors of *Mycobacterium tuberculosis* CYP121 from Indonesian natural products, *Comput. Biol. Chem*. **85**, C.

[36] D. Ramírez and J. Caballero (2018). Is it reliable to take the molecular docking top scoring position as the best solution without considering available structural data?, *Molecules* **23**, 1038.

[37] C. N. Pace, H. Fu, K. L. Fryar, J. Landua, S.R. Trevino, B.A. Shirley, M. McNutt-Hendricks, S. Iimura, K. Gajiwala, J.M. Scholtz and G.R. Grimsley (2011). Contribution of hydrophobic interactions to protein stability, *J Mol Biol*. **408**, 514-528.

[38] L. Martinez (2015). Automatic identification of mobile and rigid substructures in molecular dynamics simulations and fractional structural fluctuation analysis, *PLoS one* **10**, e0119264.

[39] X. Cheng and I. Ivanov (2012). Molecular dynamics, *Methods Mol. Biol*. **929**, 243-85.

[40] S. De Vita, M. G. Chini, G. Bifulco and G. Lauro (2021). Insights into the ligand binding to bromodomain-containing protein 9 (BRD9): a guide to the selection of potential binders by computational methods, *Molecules* **26**, 7192.

[41] A. Gavezzotti (2016). Comparing the strength of covalent bonds, intermolecular hydrogen, bonds and other intermolecular interactions for organic moleculaes: X-ray diffraction data and quantum chemical calculations, *New J. Chem*. **40**, 6848-6853.

[42] S. Thangapandian, S. John, M. Arooj and K. W. Lee (2012). Molecular dynamics simulation study and hybrid pharmacophore model development in human LTA4H inhibitor design, *PLoS one* **7**, 4.

[43] F. A. Bernal and E. Coy-Barrera. (2015). Molecular docking and multivariate analysis of xanthones as antimicrobial and antiviral agents, *Molecules* **20**, 13165-13204.

[44] K. Y. Khaw, S.B. Choi, S. C. Tan, H.A. Wahab, K. L. Chan and V. Murugaiyah (2014). Prenylated xanthones from mangosteen as promising cholinesterase inhibitors and their molecular docking studies, *Phytomedicine* **21**, 1303-1309.

[45] S. Genovese, S. Fiorito, V. A. Taddeo and F. Epifano (2016). Recent developments in the pharmacology of prenylated xanthones, *Drug Discov. Today* **21**, 1814-1819.

[46] M. Y. Ibrahim, N.M. Hashim, S. Mohan, M. A. Abdulla, S. I. Abdelwahab, B. Kamalidehghan, M. Ghaderian, F. Dehghan, L.Z. Ali, H. Karimian, M. Yahayu, G. Cheng L. Ee, A.S. Farjam and H.M.

Ali (2014). Involvement of Nf-kB and HSP-70 signaling pathways in the apoptosis of MDA-MB-231 cells induced by a prenylated xanthone compound, a-mangostin, from *Cratoxylum arborescens*, *Drug Des. Dev. Ther*. **8**, 2193–2211.

[47] S. M. Al-Massarani, A. A. El Gamal, N. M. Al-Musayeib, R. A. Monthana, O. A. Basudan, A. J. Al-Rehaily, M. Farag, M. H. Assaf, K. H. El-Tahir and L. Maes (2013). Phytochemical, antimicrobial and antiprotozoal evaluation of *Garcinia mangostana* pericarp and a-mangostin, its major xanthone derivative, *Molecules* **18**, 10599–10608.

[48] J. Ngoupayo, T. K. Tabopda and M. S. Ali (2009). Antimicrobial and immunomodulatory properties of prenylated xanthones from Garcinia staudtii, *Bioorg. Med. Chem*. **17**, 5688–5695.

A C G
publications
© 2022 ACG Publications